Structural and Magnetic Properties of a Novel Double Perovskite Sm_2MgRuO_6

I. B. M. Mouadje, R. Djoumessi Fobasso, B. Sondezi

Physics Department, University of Johannesburg, Auckland Park 2006, South Africa

E-mail: 224221523@student.uj.ac.za

Abstract. Double perovskite oxides ($A_2B'B''O_6$) have attracted significant attention due to their unique combination of functional properties. These materials are particularly promising for spintronic and energy applications, where precise control of cation ordering and magnetic interactions is critical. In this study, we synthesized the novel double perovskite Sm_2MgRuO_6 via solid-state reaction and investigated its structural and magnetic properties to understand its potential for advanced technologies. The crystal structure of Sm_2MgRuO_6 was identified by X- ray diffraction (XRD) at room temperature and Rietveld refinement confirm that the compound crystallizes in the monoclinic $P2_1/n$ space group with lattice parameters a = 5.41194 Å, b = 5.66563 Å, and c = 7.71585 Å. The structure exhibits a rock-salt-like cationic ordering of Mg^{2+} and Ru^{4+} on the octahedral sites, similar to Nd_2MgRuO_6, but with partial disorder. To elucidate the magnetic behavior, we employed Monte Carlo (MC) simulations, a powerful computational technique that uses stochastic sampling to model thermodynamic properties and phase transitions in complex systems. The MC results, based on a Heisenberg spin Hamiltonian, reveal ferromagnetic ordering driven by Sm^{3+} and Ru^{4+} interactions. This work provides crucial insights into the structure-property relationships of Sm_2MgRuO_6, highlighting its potential as a room-temperature ferromagnetic material for spintronic applications. The combination of experimental characterization and computational modeling establishes a robust framework for designing next generation functional perovskites.

1 Introduction

Double perovskites of the type $A_2B'B''O_6$, with magnetic B′ and B″ ions at the octahedral sites, have gained significant interest due to their potential for magnetoresistive and spintronic applications. Notable examples include Sr_2FeMoO_6 exhibiting room-temperature colossal magnetoresistance [1], multiferroic $Ba_2FeMnCoO_6$ [2] and Dy_2NiMnO_6 [3], and Sr_2CrIrO_6, a ferrimagnetic insulator with a record-high Curie temperature (~90 K) that can transition to half-metallicity via doping [4,5]. In contrast, systems with magnetic interactions between A- and B-site cations remain less explored. Ruthenium-based double perovskites are particularly intriguing due to the interplay between 4d electron itinerancy and strong spin-orbit coupling, leading to unique magnetic properties compared to their 3d counterparts [6]. For instance, Nd_2MgRuO_6 exhibit coupled A- and B-site spin ordering with antiferromagnetic arrangements [7], though their Ru^{5+} ions are magnetically diluted by non-magnetic Na^+/Li^+ [8–10]. However, studies on Ru^{4+} -based analogues (e.g., Ln_2NiRuO_6) are scarce, with reports of rare-earth ordering (Er, Ho) but no long-range Nd magnetism [11]. Here, we present the structural and magnetic properties of Sm_2MgRuO_6, a novel Ru^{4+} ($4d^4$) double perovskite stabilized by Mg^{2+}. The large ionic radius difference (Ru^{4+}: 0.62 Å, Mg^{2+}: 0.72 Å) drives rock-salt ordering of B-site cations, isolating Ru^{4+} and enabling weak magnetic interactions.

2 Experimental and Simulation details

2.1 Experimental method

The Sm_2MgRuO_6 polycrystalline compound was synthesized by conventional high-temperature solid-state reaction method under controlled temperature and time conditions. Stoichiometric proportions of high purity (99.99 %) Samarium (III) oxide (Sm_2O_3), Ruthenium (IV) oxide (RuO_2) and Magnesium (IV) oxide (MgO) were mixed thoroughly and heated at 800 °C for 12h. The pre-heated powders were sintered again at 1250 °C for 36h with intermediate grinding before any characterization processes could be employed. The XRD pattern with Cu-Kα radiation (λ=1.5418 Å) at room temperature shows the presence of a moderately strong superlattice reflection at 2θ ~ 19^O indicating the possibility of crystallographic ordering of the Mg and Ru cations at the perovskite B-site. Rietveld refinement using FULLPROF software indicated that Sm_2MgRuO_6 crystallizes in the monoclinic space group $P2_1/n$ that allows for a combination of rock-salt like ordering of the two B-sites. The microstructure, elements distribution and chemical compositions of Sm_2MgRuO_6 were analyzed on a scanning electron microscope (SEM) with the Energy Dispersive X-Ray Spectroscopy (EDS) options using an accelerating voltage of 20 kV.

2.2 Simulation details

We investigated the magnetic behavior using Monte Carlo (MC) methods, where random sampling of spin configurations reveals equilibrium properties and transition temperatures.

The Hamiltonian describing the system is given by:

$$H = -J_{Sm-Ru}\sum_{\langle i,j\rangle} S_i^{Sm} S_j^{Ru} \tag{1}$$

where $J_{Sm\text{-}Ru}$ is the exchange interaction between Sm-Ru, $S^{Sm} = \pm\frac{5}{2}, \pm\frac{3}{2}$ and $\pm\frac{1}{2}$ is the spin moment of Sm^{3+}, and $S^{Ru} = \pm 1$ the spin moment of Ru^{4+}.

By replacing them in eq (1), the energies for different configurations AFM and FM given by:

$$E_{AFM} = 6(\frac{5}{2})J_{Sm-Ru} \tag{2}$$

$$E_{FM} = -6(\frac{5}{2})J_{Sm-Ru} \tag{3}$$

With $E_{FM} = -3578.15960891\ \ Ry$ and $E_{AFM} = -3578.15174973\ \ Ry$

The combination of the Eqs. (2) and (3) gives the value of the coupling interaction between Sm and Ru: $J_{Sm-Ru} = \frac{E_{AFM} - E_{FM}}{12(\frac{5}{2})}$, the value of the exchange coupling between obtained by the GGA+U method is $J_{Sm-Ru} = 5.345meV$.

3 Results and Discussion

3.1 Structural Characterization

The XRD pattern of Sm_2MgRuO_6 obtained with the Rietveld refinement by the FULLPROF software [11] is plotted in **Fig. 1.**. A better fitting result with the P21/n space group is realized, and therefore the Sm_2MgRuO_6 crystalizes with monoclinic DP-type P 21/n symmetry. The refinement pattern shows phase-purity and crystallographic information of the oxide without any signature of impurity phases. The values of the reliability factors obtained from the refinement are R_{wp} = 6.4635%, R_p = 5.0538% and χ^2 = 2.89. The lattice parameters are a = 5.66563(9) Å, b = 5.66563(2) Å, c = 7.71585(6) Å and V = 236.584(9) $Å^3$.

The tolerance factor t:

$$t = \frac{r_{Sm} + r_O}{\sqrt{2}\left(\frac{r_{Mg} + r_{Ru}}{2} + r_O\right)} \quad (4)$$

where r is ionic radius, can be used to evaluate the structural stability of perovskite-type oxides [12]. A phase stability is confirmed with t ranging from 0.78 to 1.05 [13]. The value of t for Sm_2MgRuO_6 is 0.81, which also verifies the stability of DP-type crystal structure.

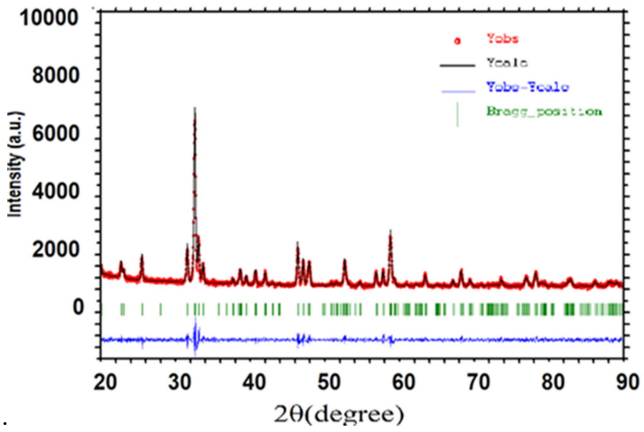

Fig. 1: Powder x-ray diffraction pattern of Sm_2MgRuO_6

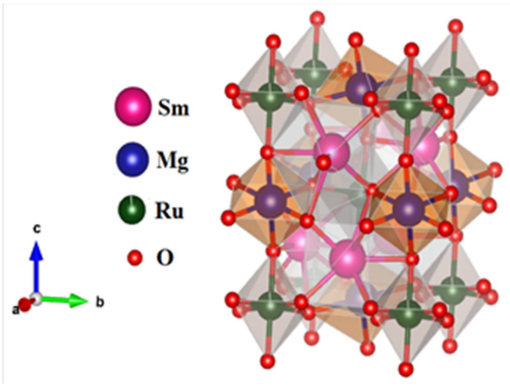

Fig. 2: $P2_1/n$ Structure

Fig. 2 illustrates the detailed crystal structure of Sm_2MgRuO_6 DP oxide and nearest neighbour environments of each element. In a single ordered unit, it has 20 independent atoms including four Sm, two Mg atoms, two Ru atoms and twelve O atoms. Both Mg and Ru atoms coordinate with six O atoms forming the MgO_6 and RuO_6 octahedrons, respectively. The bond distance ranges and average bond distance are 1.837–2.100 Å and 1.943 Å for MgO_6. The one for RuO_6 are 1.890–2.174 Å and 2.079 Å for MgO_6 and RuO_6. The O-Mg-O and O-Ru-O bond angles for MgO_6 and TiO_6 units range from 86.293° to 92.097° and 88.631° to 92.330°, respectively. Sm atom is located in the gap of MgO_6/TiO_6 octahedron forming the 8-coordination polyhedron with the bond distances from 2.279 Å to 2.755 Å. Sm atom occupies the 4e Wyckoff position., Mg and Ru ions are independent positions of 2d and 2c, while there exist three different O ions (O_1, O_2 and O_3) and they are assumed three different 4e sites.
The atomic positions of Sm, Mg Ru and O are summarized in Table 1 for Sm_2MgRuO_6 DP oxide.

Wyckoff site	Atom	x	y	z
4e	Sm	0.5152(4)	0.5605(5)	0.2462(6)
2d	Mg	1/2	0	0
2c	Ru	0	1/2	0
4e	O_1	0.0988(8)	0.4713(3)	1/4
4e	O_2	0.3207(7)	0.7281(4)	-0.0477(8)
4e	O_3	0.4048(1)	0.9698(0)	0.2641(9)

Table 1. The atomic positions of Sm_2MgRuO_6 DP oxide.

Fig. 3 illustrates the secondary electron SEM image of the typical microstructure together with the element EDS mapping results of Sm_2MgRuO_6 DP oxide. The polycrystalline nature of Sm_2MgRuO_6 is confirmed by the presence of spherical particles with agglomerations in some areas. A number of EDS mapping analysis were performed and fractions confirmed the stoichiometric compositions of 68.0 %, 15.3 %, 12.4 % and 4.4% for Sm, Ru, O and Mg

atoms (Fig.4) respectively. These values are close to the nominal atomic ratio 2:1:1:6 of synthesized Sm_2MgRuO_6 oxide.

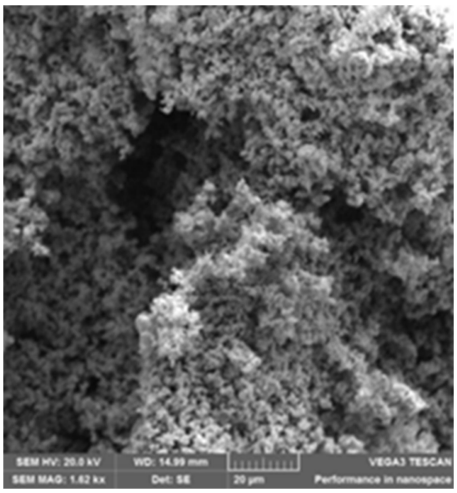

Fig. 3: SEM image

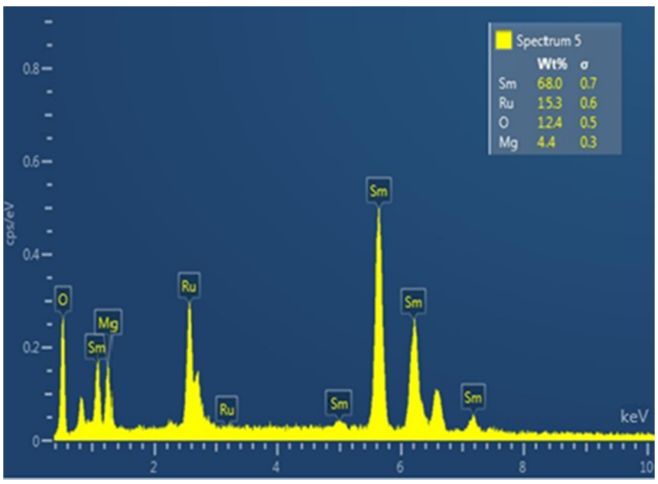

Fig. 4: EDS image

3.2 Magnetic Properties: Monte Carlo Simulation

To simulate the magnetic behavior of this complex system a MCS combined with Metropolis algorithm was performed. The system was conceived in the simulation program as a cubic bulk $L_B = 20$, which remains lower than the thermodynamic limit determined at $L_{ThL} = 32$ for this class of materials [14], [15]. An initial configuration has been randomly generated in such a way Sm-spins are located randomly in the sites of Sm-sublattice, and Ru-spins are located randomly in the sites of Ru-sublattice. At each MCS step, all the sites in the system are sequentially traversed and single-spin flip attempts are made. A Metropolis algorithm has been included in the program to help deciding the acceptance or rejection of single spin flips. The simulation has recovered the data from 5000 MCS steps, where the first 3000 steps were used to reach the equilibrium. Equations used to calculate the energy; magnetization, magnetic susceptibility (χ) and specific heat (C_V) are given respectively by:

$$E = \frac{\langle H \rangle}{N} \tag{5}$$

$$M = \frac{1}{N}\left|\sum_i S_i^{Sm} - \sum_i S_i^{Ru}\right| \tag{6}$$

$$C_V = \frac{\beta}{T}(\langle E^2 \rangle - \langle E \rangle^2) \tag{7}$$

with $\beta = \frac{1}{k_B T}$ where T is the absolute temperature, k_B is the Boltzmann constant and N is the number of spin in the system.

In order to examine the effect of the lattice size, the variation of these quantities with lattice sizes ranging from L = 12 to L = 20 were illustrated in **Figs. 5, 6** and **7**. Internal energy as a function of temperature is shown in Fig. 5. The simulated transition temperature has been found to be 275 K for small lattice sizes. When the size of the systems increases, the transition temperature reaches a peak at T_C =276.76 K.

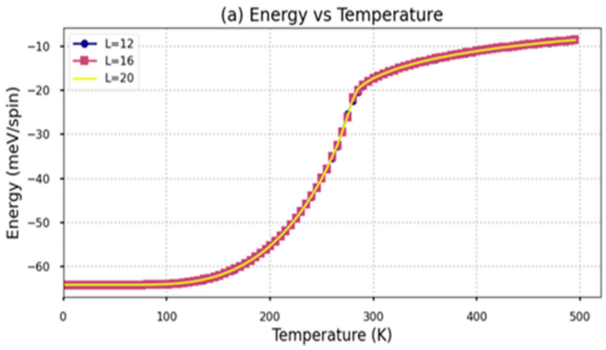

Fig.5: Internal Energy as a function of temperature for different lattice sizes

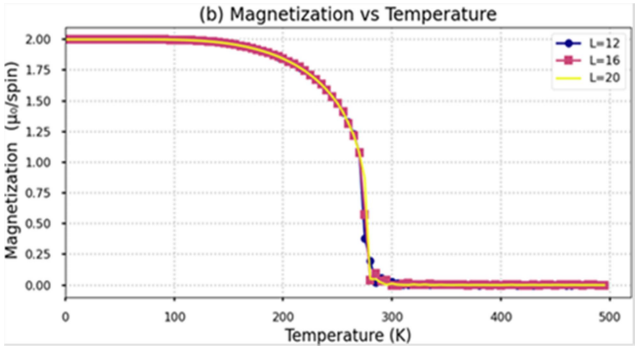

Fig.6: Total magnetization as a function of temperature for different lattice sizes

The total magnetization as function of temperature is shown in **Fig. 6** as a function of temperature. The curve reaches a magnetic saturation value of M_T =2μB. This magnetization curves tends to gradually decrease after T_C to reach the minimum value M_T = 0,15μB. Similar behavior was observed for different lattice sizes. A slight increase in critical temperature of about T_C =276.76 K were observed. The simulated specific heat as function of temperature (C_V) is shown in **Fig.7.** The transition temperature is consistently found at 275 K. For large system sizes, the transition temperature bifurcates to 276.76 K. The curve has a Gaussian form which is a sign of a second order phase transition. Results obtained show that a change in the size of the system is at the origin of a minimal variation in critical temperature T_C.

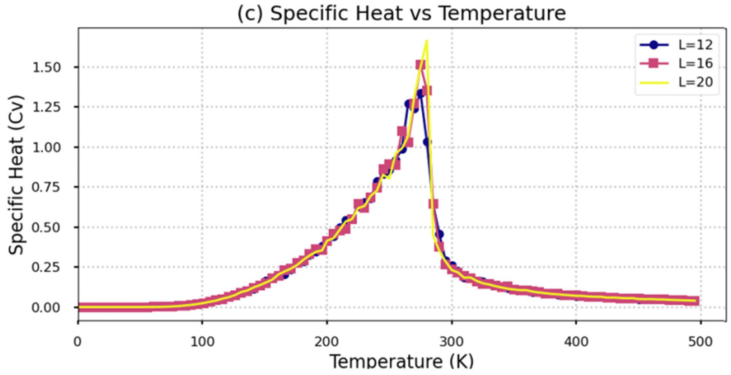

Fig.7: Specific Heat as a function of temperature for different lattice sizes

To date, the critical temperature T_C found in this present work has the lowest value compared to the majority of results reported in the literature by other authors in similar studies such as $La_{0.67}Sr_{0.33}MnO_3$ (T_C = 358 K [16]), Mn_2FeReO_6 (T_C =520 K [17]), Sr_2CrReO_6 (T_C = 610 K [18]), Sr_2CrOsO_6 (T_C = 725 K [19]), Sr_2CrMoO_6 (T_C = 458 K [20]), Sr_2CrWO_6 (T_C = 500 K [21]), Ca_2CrMoO_6 (T_C = 125 K [22]).

4 Conclusion

In summary, high quality single phased polycrystalline Sm_2MgRuO_6 oxide with a B-site ordered monoclinic P21/n (No. 14) DP type crystal structure has been successfully fabricated. A combined theoretical and experimental investigation has been carried out. The Sm_2MgRuO_6 oxide belongs to a B-site ordered monoclinic double perovskite (DP) type structure. Monte Carlo simulations confirms the Curie temperature of the Sm_2MgRuO_6 to be 276.76 K for

L= 20. There are ferromagnetic interactions between Sm^{3+} and Ru^{4+}, demonstrating how structural distortion governs its unique magnetic properties.

References

[1] K.I. Kobayashi, T. Kimura, H. Sawada, K. Terakura, Y. Tokura, Nature 395 (1998) 677–680.
[2] S. Yáñez-Vilar, E.D. Mun, V.S. Zapf, B.G. Ueland, S. Gardner, J.D. Thompson,J. Singleton, M. Sánchez-Andújar, J. Mira, N. Biskup, M.A. Señarís-Rodríguez, C.D. Batista, Phys. Rev. B 84 (2011) 134427.
[3] M.Azuma,K.Takata, T. Saito, S. Ishiwata, Y. Shimakawa, M. Takano, J. Am. Chem.Soc. 127 (2005) 8889–8892.
[4] Y. Krockenberger, K. Mogare, M. Reehuis, M. Tovar, M. Jansen, G. Vaitheeswaran, V. Kanchana, F. Bultmark, A. Delin, F. Wilhelm, A. Rogalev, A. Winkler, L. Alff, Phys. Rev. B 75 (2007) 020404.
[5] K. Samanta, P. Sanyal, T.S. Dasgupta, Sci. Rep. 5 (2015) 15010.
[6] G. Cao, A. Subedi, S. Calder, J.-Q. Yan, J. Yi, Z. Gai, L. Poudel, D.J. Singh, M.D. Lumsden, A.D. Christianson, B.C. Sales, David Mandrus, Phys. Rev. B 87 (2013) 155136.
[7] R.P. Singh, C.V. Tomy, Phys. Rev. B 78 (2008) 024432.
[8] W.R. Gemmill, M.D. Smith, H.-C. zur Loye, J. Solid State Chem. 177 (2004) 3560–3567.
[9] A.A. Aczel, D.E. Bugaris, J. Yeon, C. de la Cruz, H.-C. zur Loye, S.E. Nagler, Phys. Rev. B 88 (2013) 014413.
[10] S.J. Makowski, J.A. Rodgers, P.F. Henry, J.P. Attfield, J.W.G. Bos, Chem. Mater. 21 (2009) 264–272.
[11] J. Rodriguez-Carvajal, Laboratoire Leon Brillouin CEA-CNRS, France, 2007.
[12] C. Bartel , C. Suton , B. Goldsmith , R. Oyang , C. Musgrave , M. Schefler , Sci. Adv.
5 (2019) eaav0693.
[13] O. El Rhazouani, Z. Zarhri, A. Benyoussef, A. El Kenz, J. Mag. Mag. Mat. 401 (2016) 897.
[14] O. El Rhazouani, A. Benyoussef, A. El Kenz, J. Magn. Magn. Mat. 377 (2015) 319.
[15] A. Loudaini, M. Aggour, O. Mounkachi, L. Bahmad, Solid State Com. 295 (2019) 5–11.
[16] M. Kibbou, Y. Benhouria, M. Boujnah, I. Essaoudi, A. Ainane, R. Ahuja, J. Magn. Magn. Mater. 495 (2020) 165833.
[17] O. El Rhazouani, A. Benyoussef, Z. Zarhri, A. El Kenz, J. Magn. Magn. Mater. 401 (2016) 897–901.
[18] O. El Rhazouani, Z. Zarhri, A. Benyoussef, A. El Kenz, Phys. Lett. Sect. A: Gen. At. Solid State Phys. 380 (13) (2016) 1241–1246.
[19] O. El Rhazouani, A. Slassi, Comput. Condens. Matter 11 (2017) 55–59.
[20] O. El Rhazouani, A. Slassi, Y. Ziat, A. Benyoussef, Phys. A, Stat. Mech. Appl. 476 (2017) 38–42.
[21] O. El Rhazouani, Y. Ziat, A. Benyoussef, , Mod. Electron. Mater. 3(3) (2017) 99–103.
[22] A.S. Erchidi Elyacoubi, R. Masrour, A. Jabar, M. Ellouze, E.K. Hlil, Mater. Res. Bull. 99 (2018) 132–135.